Molecular Architecture of Oligothiophene on a Highly Oriented Pyrolytic Graphite Surface by Employing Hydrogen Bondings

Li-Ping Xu,[†] Jian-Ru Gong,[†] Li-Jun Wan,* Tong-Gang Jiu, Yu-Liang Li,* Dao-Ben Zhu, and Ke Deng*,[‡]

Beijing National Laboratory for Molecular Sciences, Institute of Chemistry, Chinese Academy of Sciences (CAS), Beijing 100080, China

Received: May 26, 2006; In Final Form: July 5, 2006

To achieve a controllable and predictable molecular architecture on a two-dimensional (2D) surface, a series of oligothiophenes with carboxylic groups and alkane chains were synthesized. The alkane chains and carboxylic groups, which can form hydrogen bonding, were intentionally designed in different positions of the oligothiophenes. The resulted molecular architectures by using the so-prepared oligothiophenes on a highly oriented pyrolytic graphite (HOPG) surface were investigated by scanning tunneling microscopy (STM) and density functional theory (DFT). It is found that the hydrogen bonding plays an essential role in the formation of the ordered assemblies. A controlled 2D molecular assembly could be fabricated by using hydrogen bondings.

1. Introduction

Self-assembly is a spontaneous process involved in functional materials and living organisms[1] and an effective approach to fabricate a variety of nanostructures as a "bottom-up" strategy in nanofabrication.[2−6] The formation of a self-assembly is usually dominated by weaker noncovalent intermolecular actions such as hydrogen bonding, van der Waals interaction, and $\pi-\pi$ interaction.[7] Therefore, understanding and employing the weaker interactions is an important issue in designing assembly, making an artificial organism, and fabricating a molecular device. Among the various intermolecular reactions, hydrogen bondings exist well in the nature from the double helix of DNA to the bonding of H_2O molecules in liquid water. Because of their high selectivity and directionality, hydrogen bonding plays an important role in the formation of 2D self-assembly on a solid surface.[8−17] Owing to the flexibility, hydrogen bondings have been often observed in 2D self-assembly. As a result of the intensive study, it is known that hydrogen bonding can be formed through H···O···H, H···N···H, and H···F···H in 2D or 3D assemblies.[8−22] In previous studies, the effort was usually made to find the existence of hydrogen bondings in a self-assembly. The molecules with hydrogen bondings can form different networks that are employed as templates to fabricate host−guest assemblies with other molecules.[23−26] However, an intentionally designed assembly by employing hydrogen bondings is rarely reported. It is a challenge to detect the possibility to fabricate a controllable and/or predictable molecular architecture with noncovalent weaker intermolecular reactions, which is the prerequisite for the practical application of self-assembly instead of natural products.

Owing to high conductivity and environmental stability, conjugated polymers are promising candidates in many electronic devices such as light-emitting diodes,[27] thin film field-effect transistors,[28] solid-state lasers,[29] and photovoltaic devices.[30] In particular, polythiophene and its substituted derivatives seem to be of great interest. In the case of poly(3-hexylthiophene), the field-effect mobility as high as 0.1 $cm^2\ V^{-1}\ s^{-1}$ has been measured. On the other hand, it has been demonstrated that the performance of a device is highly dependent on the perfection of the structural organization.[31] For example, solid-state quantum efficiencies were found to be related to the degree of long-range order in the conjugated polymers and nonemissive orientation is significant in materials with a greater degree of long-range order.[32]

In the present paper, we report how to employ hydrogen bondings to make molecular assemblies. The relationship between the formation of oligothiophene self-assembly and hydrogen bondings is investigated. A series of oligothiophenes with carboxylic groups and alkane chains were designed and synthesized.[33] Hydrogen bondings induced from carboxylic groups were intentionally designed in different positions of the oligothiophene molecules. Various self-assemblies from the so-prepared oligothiophenes were deposited on an HOPG surface and studied by scanning tunneling microscopy (STM) and density functional theory (DFT). The hydrogen bonding was found to play an essential role in the formation of the assemblies. Under the assistance of hydrogen bondings, long-range ordered molecular architectures were achieved. The symmetry and molecular arrangement in the assemblies can be controlled and predicted from the hydrogen bonding.

2. Experimental and Computational Details

Four compounds of different thiophene units (TA, 3-thiophene acetic acid; DTDA, 2,2′-bithiophene-5,5′-dicarboxylic acid; TTDA, 3′-pentyl-5,2′:5′,2″-terthiophene-2,5″-dicarboxylic acid; QTDA, 4′,3″-dipentyl-5, 2′:5′,2″:5″,2‴-quaterthiophene-2,5‴-dicarboxylic acid) were synthesized according to the procedure in the literature.[33] The chemical structures of the four compounds are shown in Chart 1.

The structural difference in the four oligothiophene molecules can be seen in Chart 1. For TA and DTDA, one and two carboxylic acid groups are attached to thiophene and bithiophene,

* To whom correspondence should be addressed. Fax: +86-10-62558934. E-mail: wanlijun@iccas.ac.cn.
[†] Also in CAS Graduate school.
[‡] National Center for Nanoscience and Nanotechnology, Beijing 100080, China.

10.1021/jp063240v CCC: $33.50
Published on Web 08/09/2006

CHART 1

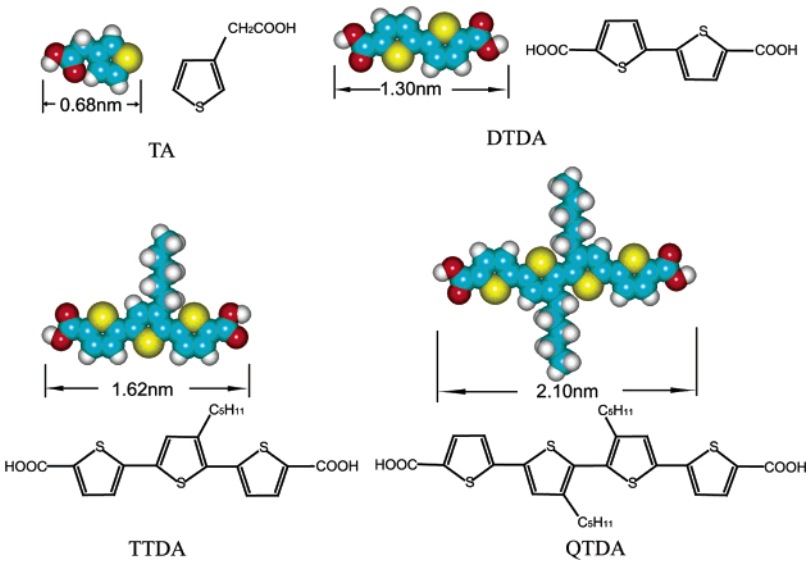

respectively. Besides two carboxylic acid groups, pentyl-alkane chains can be seen on the sides of TTDA and QTDA. In the elegant configuration of the oligothiophenes, hydrogen bondings may be formed among molecules. The pentyl-alkane chains will balance the skeleton in the later two molecules. It is clear that the intentionally designed hydrogen bonding should play an important role in the formation of self-assemblies. Those designed molecules could be used to prepare the controlled molecular architectures such as molecular dimer, wire, square, rectangle, and parallelogram. The details on the resulted molecular architectures were directly observed by STM.

The self-assembled monolayers (SAMs) of the compounds were prepared by placing a drop (ca. 2 μL) of solution containing the oligothiophene (the concentration is ca. 10^{-5} M) on a freshly cleaved atomically flat surface of HOPG (ZYB quality) with an area of about 30 mm^2. The solvent for preparing all solutions was tetrahydrofuran (THF) (Aldrich). The samples were investigated after the solvent evaporated.

A Nanoscope IIIa SPM (Digital Instruments, Santa Barbara, CA) was employed to carry out the STM experiments using a standard constant-current mode under ambient condition. STM tips were mechanically cut Pt/Ir wire (90/10). All the STM images are presented in the paper without further processing. The tunneling conditions used are given in the corresponding figure captions.

The theoretical simulation was performed by using density functional theory[34] provided by the DMol3 code. The Perdew and Wang parametrization[35] of the local exchange-correlation energy was applied in the local spin density approximation (LSDA) to describe exchange and correlation. The all-electron spin-unrestricted Kohn−Sham wave functions were expanded in a local atomic orbital basis. In the double-numerical basis set, the valence s and p orbitals were represented by two basis functions and the d type wave function on each atom was used to describe polarization. All calculations were all-electron ones and performed with the Extra-Fine mesh. A self-consistent field procedure was performed with a convergence criterion of 10^{-5} au on the energy and electron density.

3. Results and Discussion

3.1. TA. The intermolecular reaction and molecular/substrate interaction is important in dominating the formation of an assembly on a solid surface. The balance in the various interactions as well as the underlying substrate crystallization will decide the adsorption and symmetry of an adlayer.[5f,9b] Owing to the weak interaction between thiophene molecules and HOPG surface, no ordered adlayer of thiophene was reported. Although the TA molecule has a carboxylic acid group, it is not sure if an ordered adlayer could be formed.

However, a dimeric structure would be expected due to the possibility of forming hydrogen bondings between carboxylic acid groups. STM observation revealed the resulting structure on the HOPG surface.

Figure 1 is a typical STM image recorded in the TA adlayer. It can be seen that no long-range ordered structure exists on the adlayer. A careful observation found that the adlayer is composed of bright spots showing in the upper right inset in Figure 1. From the high-resolution STM image, it is clear that the bright spot appears in an elliptical shape. On the basis of the chemical structure and dimension of a TA molecule, the ellipse is assigned to a thiophene dimer circled in the upper right inset. The hydrogen bondings are expected to be responsible for the formation of the ellipse dimer. A structural model for the dimer is proposed in the lower right inset. A theoretical simulation shows that two strong hydrogen bondings can be

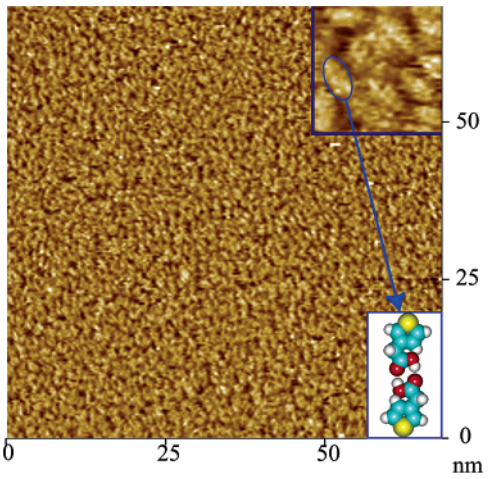

Figure 1. STM top view of a large-scale TA assembly on the HOPG surface recorded with $E_{bias} = 664$ mV, $I = 1.08$ nA. The upper inset is the high-resolution STM image of TA molecules, and the circled dimer is depicted by the molecular model in the lower inset.

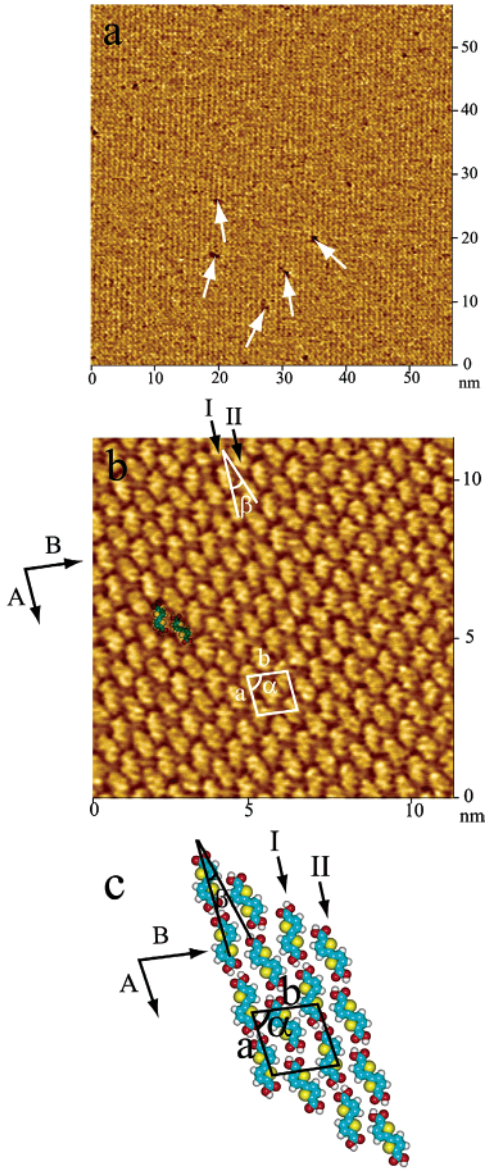

Figure 2. (a) STM top view of DTDA assembly recorded with E_{bias} = 842 mV, I = 968 pA. The arrows indicate the molecular defects in the image. (b) High-resolution STM image of DTDA molecules recorded with E_{bias} = 953 mV, I = 911 pA. (c) Structural model for the 2D packing of DTDA molecules.

really formed between the carboxyl groups of two thiophene molecules with the dissociation energy of about 31.1 kcal mol^{-1}. This strong hydrogen bonding interaction results in the dimeric structure even after being stored for a month or longer time.

3.2. DTDA. With two carboxylic acid groups and two thiophene rings, DTDA molecules have stronger intermolecular and molecular/substrate reactions than those from TA molecules. The molecules are expected to form molecular wire with a 2D ordered assembly.

Figure 2a is a typical STM image of a DTDA adlayer on an HOPG surface. It is found that the molecules form a self-assembly. Although several defects indicated by arrows can be resolved in the adlayer, a long-range ordering can be clearly seen in the image. Even in a scanning area of 100 nm × 100 nm, only one molecular domain is observed. Figure 2b is a high-resolution STM image. In this image, each DTDA molecule appears as a bright ellipse. In direction **A**, the molecules are in the same orientation. However, two adjacent molecular rows adopt a different orientation in direction **B**. Therefore, there are

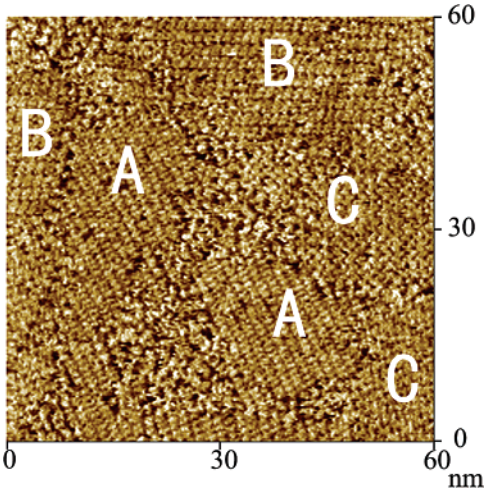

Figure 3. STM top view of TTDA assembly recorded with E_{bias} = 837 mV, I = 785 pA. **A**, **B**, and **C** indicate three domains.

two types of molecular rows, I and II. In row I, the molecules form a straight line, while a zigzag line can be seen in row II. An angle of $\beta = 16 \pm 2°$ exists between the axis of molecules in row I and row II. According to the molecular orientation and adlayer symmetry, a unit cell for the assembly can be outlined in Figure 2b. The unit cell parameters a and b, parallel to direction **A** and **B**, are measured to be distances 1.2 ± 0.1 nm and 1.1 ± 0.1 nm, respectively. The angle between **A** and **B** is 81 ± 2°. According to the STM observation, a corresponding molecular model is tentatively proposed in Figure 2c. DFT calculations have been performed to understand the bonding properties of the DTDA networks. It is found that each DTDA molecule along direction **A** is strongly hydrogen bonded with the head-to-head configuration through the carboxyl groups, with the dissociation energy of about 30.5 kcal mol^{-1} from a theoretical simulation result, although the angles of the hydrogen bondings in the neighboring molecular rows along direction **A** are different. On the other hand, along direction **B**, two types of weak hydrogen bondings, C−H···O and O−H···S, could exist between the molecular stripes, with the dissociation energy of about 4.5 kcal mol^{-1}. The intrastripe and interstripe interactions stabilize the 2D assembly. The DFT theoretical data support the experimental result. The DTDA molecules first connect with each other through the hydrogen bondings of carboxyl groups to form a molecular stripe and then organize into a domain by the week interaction between the stripes. The proposed model in Figure 2c is in good agreement with the results from STM observation. The results are consistent with the expected structure although there is a difference in the molecular orientation between row I and row II, which shows the flexibility and complexity of hydrogen bonds.

3.3. TTDA. TTDA has a complicated molecular structure compared with TA and DTDA molecules. There are more possibilities to form different molecular networks such as a square and parallelogram.

Figure 3 is an STM image of a 2D adlayer formed by TTDA on HOPG. Three types of ordered packing geometries marked by **A**, **B**, and **C** in the large-scale STM image can be seen in Figure 3. At the domain boundary, the molecules are disorderly dispersed as reported in the literature.[36] The details of each molecular domain are intensively investigated by using high-resolution STM images.

Figure 4 shows the details of the domain **A**. It can be seen that all molecules form ordered assembly. The molecular rows are clearly resolved. The high-resolution STM image in Figure

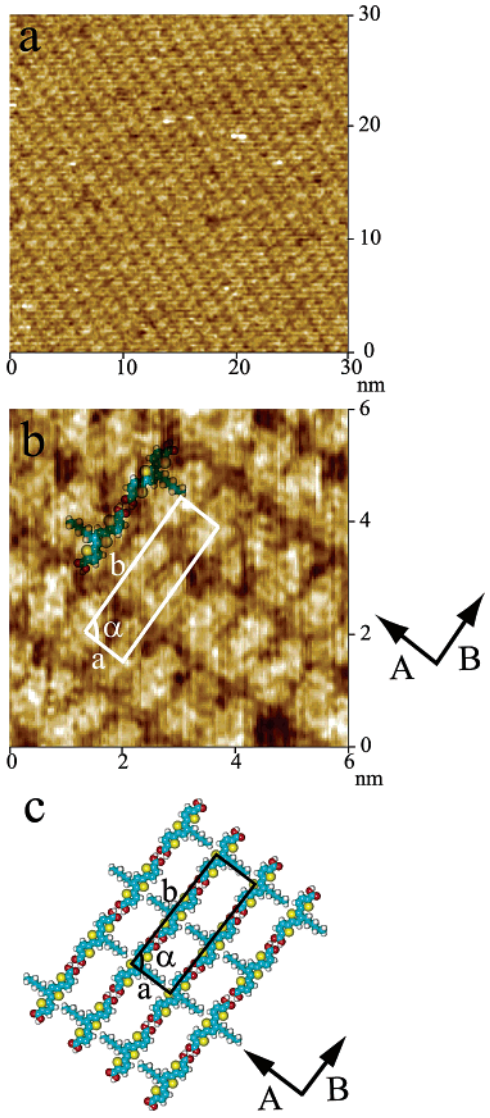

Figure 4. (a) STM top view of TTDA assembly in domain **A** recorded with $E_{bias} = 990$ mV, $I = 485$ pA. (b) The high-resolution STM image recorded with $E_{bias} = 865$ mV, $I = 696$ pA. (c) Structural model for the 2D molecular packing of TTDA molecules.

4b shows the details of the adlayer. Each molecule can be discerned as indicated by the molecular model in Figure 4b. A rectangular unit cell for the adlayer is defined in the image. The parameters of the unit cell are measured to be $a = 1.2 \pm 0.1$ nm, $b = 3.4 \pm 0.1$ nm, and $\alpha = 90 \pm 2°$. A structural model for the adlayer is proposed in Figure 4c. It can be seen in the model that the molecules form a rectangular structure through hydrogen bondings and pentyl chains. For this TTDA patterning, the theoretical result indicates that TTDA molecules tend to form head-to-head TTDA rows first, then the rows self-organize into ordered 2D assembly. The TTDA molecules in the head-to-head rows interact with each other by two strong hydrogen bondings at the end of carboxylic groups, with a dissociation energy of about 30.5 kcal mol^{-1}. In the network, two kinds of hydrogen bondings are formed among the TTDA rows. Along direction **A** of the unit cell (Figure 4c), the methyl group and the S atom formed C−H···S hydrogen bonding. Along direction **B**, the end carboxylic groups formed O−H···O hydrogen bonding. The energy of the O−H···O hydrogen bonds is very strong (about 30.5 kcal mol^{-1}), while the C−H···S hydrogen bonds is relative weak (about 3.7 kcal mol^{-1}).

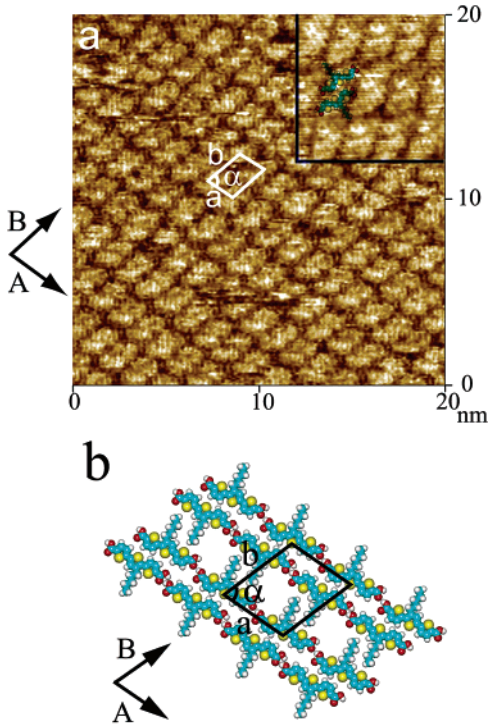

Figure 5. (a) STM top view of TTDA assembly in domain **B** recorded with $E_{bias} = 961$ mV, $I = 528$ pA, and the inset is the high-resolution STM image. (b) Structural model for the 2D packing of TTDA molecules.

For domain **B** in Figure 3, the details are revealed in a high-resolution STM image of Figure 5a. The adlayer consists of regularly molecular rows. A higher resolution STM image is shown in the upper right inset in the figure. Each molecule can be corresponded in the inset as illustrated by molecular model. On the basis of the adlayer symmetry and periodicity, a unit cell for the adlayer is outlined in Figure 5a. The parameters of the unit cell are measured to be $a = 1.6 \pm 0.2$ nm, $b = 2.2 \pm 0.2$ nm, and $\alpha = 75 \pm 2°$. Figure 5b shows the theoretical molecular packing model with calculated parameters of $a = 1.7 \pm 0.2$ nm, $b = 2.1 \pm 0.2$ nm, and $\alpha = 73 \pm 2°$ consistent with the STM measurement. In this adlayer, TTDA molecules form dimers, as illustrated in the molecular model. The TTDA dimer is connected by weak hydrogen bonding C−H···S (about 3.2 kcal mol^{-1}) through the thiophene rings. In the 2D assembly, along direction **B**, the TTDA dimers also interact with each other by weak hydrogen bondings through the alkyl side chains and thiophene rings (about 2.6 kcal mol^{-1}), while along direction **A**, the TTDA dimers interact with each other by the strong hydrogen bondings through the end carboxylic groups (about 27 kcal mol^{-1}). The balance of the bondings stabilize the adlayer on the HOPG surface and make symmetry difference from that in domain **A** as shown in Figure 4.

The molecules form an assembly with strips in domain **C**. Figure 6a is a typical STM image recorded from domain **C**. The molecular structure is obviously different from those in domains **A** and **B**. The molecules form regular stripes. In a stripe, a "Λ" shape arrangement can be seen. An individual molecule can be resolved in the image. A high-resolution STM image in Figure 6b reveals the details of the assembly. The "Λ" configuration consists of two TTDA molecules crossing each other at an angle of about $\theta = 100 \pm 2°$. A unit cell is determined for the adlayer. The measured parameters of the unit cell from STM image are $a = 1.8 \pm 0.1$ nm, $b = 3.4 \pm 0.1$ nm, and $\alpha = 90 \pm 2°$. A structural model is tentatively proposed

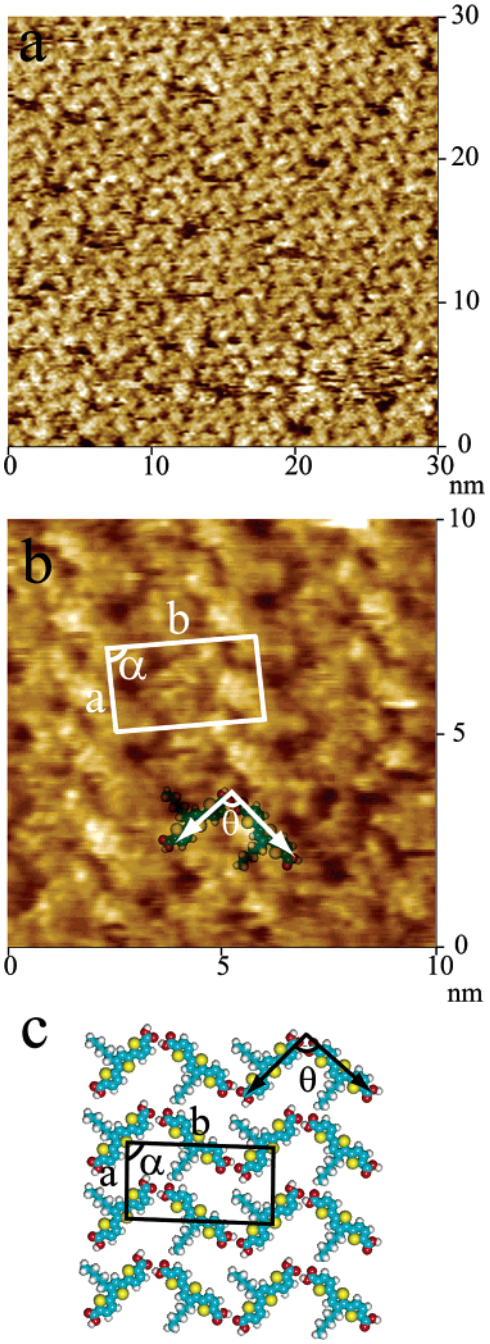

Figure 6. (a) STM top view of a larger-scale TTDA assembly in domain **C** recorded with $E_{bias} = 869$ mV, $I = 600$ pA. (b) The high-resolution STM image recorded with $E_{bias} = 869$ mV, $I = 600$ pA. (c) Structural model for the 2D molecular packing of TTDA molecules.

in Figure 6c. In the unit cell, two TTDA molecules in a "Λ" interact with each other with the hydrogen bondings through the end carboxylic group. The dissociation energy of the bonding is about 11.7 kcal mol^{-1}. To constitute the networks, adjacent molecular rows also form hydrogen bondings with the dissociation energy of 12.7 kcal mol^{-1}.

According to the theoretic calculation, the unit cell bonding energies of phases A, B, and C are 64.91, 56.14, and 26.67 kcal/mol, respectively (see Table 1). From the energy comparison of the theoretical computation, it could be concluded that the arrangement in domain A is the most stable. The arrangement in domain C arrangement is the most unstable. The STM observation also shows that only domain A exists on the surface after a week, indicating a structural transformation from unstable to stable. The results are further supported by the theoretical computation.

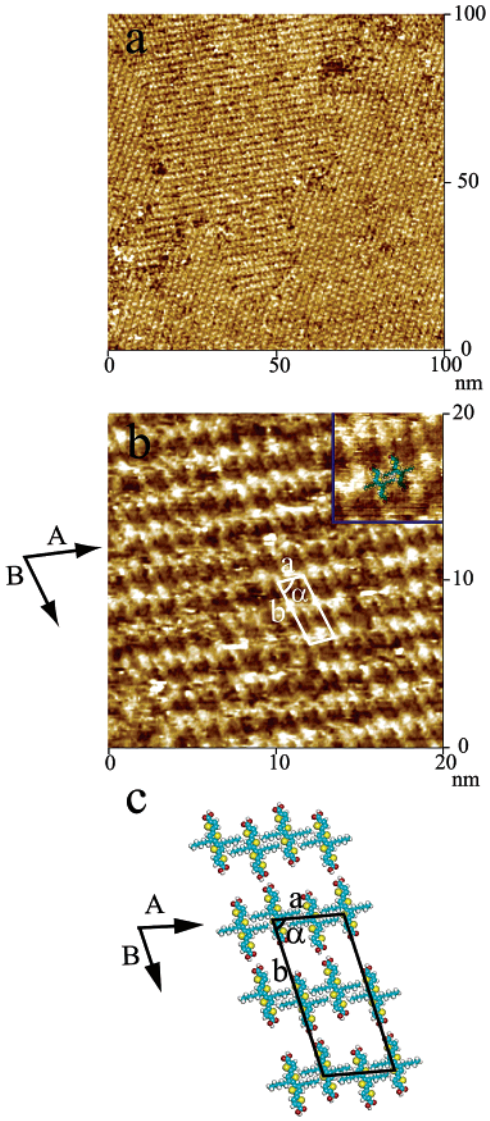

Figure 7. (a) STM top view of a large-scale QTDA assembly recorded with $E_{bias} = 886$ mV, $I = 553$ pA. (b) The STM image of QTDA with a superimposed molecular model and the high-resolution image in the inset. (c) Structural model for the 2D packing of QTDA molecules.

TABLE 1: Molecular Packing Density, Theoretical Energy, and Parameter of Unit Cells for Different Phases of the TTDA Adlayer on HOPG

	molecuar packing density (mol/nm^2)	theoretical energy (kcal/mol)	parameter of unit cell
A	0.49	64.91	$a = 1.2 \pm 0.1$ nm, $b = 3.4 \pm 0.1$ nm, $\alpha = 90 \pm 2°$
B	0.59	56.14	$a = 1.6 \pm 0.2$ nm, $b = 2.2 \pm 0.2$ nm, $\alpha = 75 \pm 2°$
C	0.33	26.67	$a = 1.8 \pm 0.1$ nm, $b = 3.4 \pm 0.1$ nm, $\alpha = 90 \pm 2°$

3.4. QTDA. QTDA has a similar molecular structure to TTDA. However, in addition to quaterthiophene rings, there are two alkyl chains forming a balance in the two sides of the molecular skeleton. A stable and ordered 2D QTDA molecular network on the HOPG surface is expected.

As shown in Figure 7a, QTDA molecules form a long-range ordered 2D network. Several domains can be seen in the image

with identical molecular arrangement. The molecular rows in each domain are clear. A high-resolution STM image in Figure 7b shows the details of the assembly. It was reported that the π systems appear much brighter than alkyl chains in STM images.[34] The bright moieties in the image are attributed to the quaterthiophene units. The high-resolution STM image in the upper right inset shows a displacement of neighboring molecules in a molecular row. The corresponding model for the molecular displacement is superimposed in the inset of Figure 7b. It is clear that the difference in molecular structure results in the difference in the 2D assembly. Molecules form ordered rows in directions **A** and **B**. The periodicities of the 2D assembly in the **A** and **B** directions are measured to be $a = 2.4 \pm 0.1$ nm and $b = 4.7 \pm 0.1$ nm, respectively. The angle between the **A** and **B** directions is $\alpha = 78 \pm 2°$. A unit cell is outlined in Figure 7b. On the basis of the STM observation, a structural model for the 2D packing of QTDA molecules is proposed in Figure 7c. The unit cell parameters for the adlayer from theoretical simulation are $a = 2.5 \pm 0.1$ nm, $b = 4.8 \pm 0.1$ nm, and $\alpha = 78 \pm 2°$ in good agreement with the experimental data. In direction **A**, the molecules lie parallel to each other and form the molecular rows through the interdigitation of the alkyl side chains with a bonding energy of about 5.1 kcal mol^{-1}. Owing to the interdigitation, a position displacement exists between the neighboring thiophene skeletons. In direction **B**, QTDA molecules interact by hydrogen bondings between carboxylic groups alternately, with a dissociation energy of about 30.4 kcal mol^{-1}. This arrangement is favorable to form a long-range ordered adlayer with the highly stability even after a month.

For all the molecules, the hydrogen bonding plays an important role in the monolayer formation. However, the molecular structure such as symmetry and alkyl chains is also responsible for the assembly formation. Different molecular adsorption structures of the four compounds could be attributed to their different molecular structures and symmetries. Compared with TA, the symmetrical disubstitution of carboxylic end groups in DTDA makes the molecule have higher symmetry and enhances the intermolecular interaction stronger. Therefore, more ordered packing of DTDA than that of TA is observed. The 2D architecture is composed of molecular lines. Because of an asymmetric chemical structure, the TTDA adlayer is complicated. STM images reveal three types of adsorption geometries for TTDA at the initial assembling stage. The molecules form rectangle, "Λ" shape, and parallelogram networks, although a stable adlayer was finally obtained. For QTDA, the symmetric chemical structure dominates the 2D network. Hydrogen bondings and alkyl side chain interdigitation stabilize and balance the adlayer with a defined structure, forming a framework in the long-range well-ordered molecular packing. The expected architectures such as molecular dimer, line, square, rectangle, and parallelogram in the four compounds really exist in their corresponding 2D networks. The results in the present research demonstrate the possibility to predict and fabricate a molecular architecture by employing hydrogen bondings and should be significant in the study of chemical self-assembly.

4. Conclusion

In summary, various molecular architectures such as molecular dimer, line, square, rectangle, and parallelogram have been fabricated by designed molecules. STM observation revealed the structural details of the architectures. From the experimental and DFT results, it is found that the hydrogen bonding plays an essential role in forming the assemblies although molecular symmetry in their chemical structure is also important. By an intentional design, molecules with hydrogen bondings can be formed into different 2D self-assemblies on a solid surface. These results suggest a feasible approach to the construction of a wide range of suparmolecular architectures through molecular engineering. Self-assembly could be adjusted by the grafting of appropriate chemical substituents, which leads to a remarkable improvement of the structural organization of molecules at the molecular level. The ordered assembly on the nanometer scale could be a crucial step for the realization of molecular nanodevices.

Acknowledgment. This work was partly supported by the National Natural Science Foundation of China (Nos.: 20025308, 20177025, 20121301, and 90406024), Chinese Academy of Sciences, and National Center for Nanoscience and Nanotechnology.

References and Notes

(1) (a) Gross, M. *Travels to the Nanoworld: Miniature Machinery in Nature and Technology*; Plenum: New York, 1999. (b) *Molecular Electronics*; Jortner, J., Ratner, M., Eds.; IUPAC Chemistry for the 21st Century Monographs; Blackwell Science: Oxford, U.K., 1997.

(2) Whitesides, G. M.; Mathias, J. P.; Seto, C. T. *Science* **1991,** *254*, 1312.

(3) Joachim, C.; Gimzewski, J. K.; Aviram, A. *Nature* **2000**, *408*, 541.

(4) Cheng, J. Y.; Mayes, A. M.; Ross, C. A. *Nat. Mater*. **2004**, *3*, 823.

(5) (a) Xu, S.; Szymanski, G.; Lipkowski, J. *J. Am. Chem. Soc.* **2004**, *126*, 12276. (b) Soto, J. E.; Kim, Y. G.; Chen, X.; Park, Y. S.; Soriaga, M. P. *J. Electroanal. Chem.* **2001**, *500*, 374. (c) Esplandiu, M. J.; Hagenstrom, H.; Kolb, D. M. *Langmuir* **2001**, *17*, 828. (d) Yamada, R.; Uosaki, K. *Langmuir* **1997**, *13*, 5218. (e) Wan, L. J.; Itaya, K. *J. Electroanal. Chem.* **1999**, *473*, 10. (f) Wan, L. J.; Wang, C.; Bai, C. L.; Osawa, M. *J. Phys. Chem B* **2001,** *105*, 8399.

(6) (a) Xu, Q. M.; Wang, D.; Wan, L. J.; Wang, C.; Bai, C. L.; Feng, G. Q.; Wang, M. X. *Angew. Chem., Int. Ed.* **2002**, *41*, 3408. (b) Pan, G. B.; Liu, J. M.; Zhang, H. M.; Wan, L. J.; Zheng, Q. Y.; Bai, C. L. *Angew. Chem., Int. Ed.* **2003**, *42*, 2747. (c) Gong, J. R.; Wan, L. J.; Yuan, Q. H.; Bai, C. L.; Jude, H.; Stang, P. J. *Pro. Natl. Acad. Sci.* USA **2005,** *102*, 971. (d) Yuan, Q. H.; Wan, L. J.; Hershel, J.; Stang, P. J. *J. Am. Chem. Soc.* **2005**, *127*, 16279.

(7) Lehn, J. M. *Supramolecular Chemistry: Concept and Perspectives;* VCH: Weinheim, Germany, 1995.

(8) Barth, J. V.; Weckesser, J.; Cai, C.; Günter, P.; Bürgi, L.; Jeandupeux, O.; Kern, K. *Angew. Chem., Int. Ed.* **2000,** *39*, 1230.

(9) (a) De Feyter, S.; De Schryver, F. C. *J. Phys. Chem. B* **2005**, *109*, 4290. (b) Wan, L. J. *Acc. Chem. Res.* **2006,** *39*, 334.

(10) (a) Otero, R.; Schöck, M.; Molina, L. M.; Lœgsgaard, E.; Stensgaard, I.; Hammer, B.; Besenbacher, F. *Angew. Chem., Int. Ed.* **2005,** *44*, 2270. (b) Yoshimoto, S.; Yokoo, N.; Fukuda, T.; Kobayashi N.; Itaya K. *Chem. Commun*. **2006**, 500. (c) Yablon, D. G.; Wintgens, D.; Flynn, G. W. *J. Phys. Chem. B* **2002**, *106*, 5470.

(11) Tao, F.; Bernasek, S. L. *J. Am. Chem. Soc.* **2005,** *127*, 12750.

(12) Vidal, F.; Delvigne, E.; Stepanow, S.; Lin, N.; Barth, J. V.; Kern, K. *J. Am. Chem. Soc.* **2005,** *127*, 10101.

(13) Keeling, D. L.; Oxtoby, N. S.; Wilson, C.; Humphry, M. J.; Champness, N. R.; Beton, P. H. *Nano Lett.* **2003**, *3*, 9.

(14) (a) Lackinger, M.; Griessl, S.; Markert, T.; Jamitzky, F.; Heckl, W. M. *J. Phys. Chem B* **2004,** *108*, 13652. (b) Lackinger, M.; Griessl, S.; Heckl, W. M.; Hietschold, M.; Flynn, G. W. *Langmuir* **2005**, *21*, 4984.

(15) Chen, Q.; Richardson, N. V. *Nat. Mater.* **2003,** *2*, 324.

(16) Yan, H. J.; Lu, J.; Wan, L. J.; Bai, C. L. *J. Phys. Chem B* **2004,** *108,* 11251.

(17) (a) Xu, L. P.; Yan, C. J.; Wan, L. J.; Jiang, S. G.; Liu, M. H. *J. Phys. Chem. B* **2005,** *109*, 14773. (b) Noda, H.; Wan, L. J.; Osawa, M. *Phys. Chem. Chem. Phys.* **2001**, *3*, 3336.

(18) Prins, L. J.; Reinhoudt, D. N.; Timmerman, P. *Angew. Chem., Int. Ed.* **2004,** *40*, 2382.

(19) Thalladi, V. R.; Weiss, H. C.; Blalser, D.; Boese, R.; Nangia, A.; Desiraju, G. R. *J. Am. Chem. Soc.* **1998**, *120*, 8702.

(20) Sureshan, K. M.; Murakami, T.; Miyasou, T.; Watanabe, Y. *J. Am. Chem. Soc.* **2004**, *126*, 9174.

(21) Park, J. S.; Lee, G. S.; Lee, Y.-J.; Park, Y. S.; Yoon, K. B. *J. Am. Chem. Soc.* **2002**, *124*, 13366.

(22) Vicente, V.; Martin, J.; Jimenez-Barbero, J.; Chiara, J. L.; Vicent, C. *Chem.−Eur. J.* **2004**, *10*, 4240.
(23) Stepanow, S.; Lingenfelder, M.; Dmitriev, A.; Spillmann, H.; Delvigne, E.; Lin, N.; Deng, X. B.; Cai, C. Z.; Barth, J. V.; Kern, K. *Nat. Mater.* **2004**, *3*, 229.
(24) Lu, J.; Lei, S. B.; Zeng, Q. D.; Kang, S. Z.; Wang, C.; Wan, L. J.; Bai, C. L. *J. Phys. Chem. B* 2004, *108*, 5161.
(25) Wu, D. X.; Deng, K.; Zeng, Q. D.; Wang, C. *J. Phys. Chem. B* **2005,** *109*, 22296.
(26) Theobald, J. A.; Oxtoby, N. S.; Phillips, M. A.; Champness, N. R.; Beton, P. H. *Nature* **2003**, *424*, 1029.
(27) Berggren, M.; Inganäs, O.; Gustafsson, G.; Rasmusson, J.; Andersson, M. R.; Hjertberg, T.; Wennerström, O. *Nature* **1994**, *372*, 444.
(28) Burroughes, J. H.; Jones, C. A.; Friend, R. H. *Nature* **1988**, *335*, 137.
(29) Hide, F.; Diaz-Garcia, M. A.; Schwartz, B.; Andersson, M. R.; Pei, Q.; Heeger, A. J. *Science* **1996**, *273*, 1833.
(30) Halls, J. J. M.; Walsh, C. A.; Greenham, N. C.; Marseglia, E. A.; Friend, R. H.; Moratti, S. C.; Holmes, A. B. *Nature* **1995**, *376*, 498.
(31) Sirringhaus, H.; Brown, P. J.; Friend, R. H.; Nielsen, M. M.; Bechgaard, K.; Langeveld-Voss, B. M. W.; Spiering, A. J. H.; Janssen, R. A. J.; Meijer, E. W.; Herwig, P.; De Leeuw, D. M. *Nature* **1999**, *401*, 685.
(32) Weder, C.; Wrighton, M. S. *Macromolecules* **1996**, *29*, 5157.
(33) Jiu, T. G.; Liu, H. B.; Gan, H. Y.; Li, Y. L.; Xiao, S. Q.; Li, H. M.; Liu, Y.; Lu, F. S.; Jiang, L.; Zhu, D. B. *Synth. Met.* **2005**, *148*, 313.
(34) Zhang, R. Q.; Wong, N. B.; Lee, S. T.; Zhu, R. S.; Han, K. L. *Chem. Phys. Lett.* **2000**, *319*, 213.
(35) Perdew, J. P.; Wang, Y. *Phys. Rev. B* **1992**, *45*, 13244.
(36) Gong, J. R.; Lei, S. B.; Wan, L. J.; Deng, G. J.; Fan, Q. H.; Bai, C. L. *Chem. Mater.* **2003**, *15*, 3098.